Journal of Molecular and Cellular Cardiology 46 (2009) 268–277

Contents lists available at ScienceDirect

Journal of Molecular and Cellular Cardiology

journal homepage: www.elsevier.com/locate/yjmcc

Original article

Proteomic and metabolomic analysis of cardioprotection: Interplay between protein kinase C epsilon and delta in regulating glucose metabolism of murine hearts

Manuel Mayr [a,*], David Liem [d], Jun Zhang [d], Xiaohai Li [d], Nuraly K. Avliyakulov [d], Jeong In Yang [d], Glen Young [d], Tom M. Vondriska [d], Christophe Ladroue [c], Basetti Madhu [b], John R. Griffiths [b], Aldrin Gomes [d], Qingbo Xu [a], Peipei Ping [d]

[a] Cardiovascular Division, BHF Centre, King's College, London, 125 Coldharbour Lane, London SE5 9NU, UK
[b] Cancer Research UK Cambridge Research Institute, Cambridge, UK
[c] University of Warwick, UK
[d] Department of Physiology, David Geffen School of Medicine, UCLA, Los Angeles, US

ARTICLE INFO

Article history:
Received 13 April 2008
Received in revised form 29 September 2008
Accepted 2 October 2008
Available online 26 October 2008

Keywords:
Proteomics
Metabolism
Cardioprotection
Protein kinase C
Mitochondria
Preconditioning

ABSTRACT

We applied a combined proteomic and metabolomic approach to obtain novel mechanistic insights in PKCε-mediated cardioprotection. Mitochondrial and cytosolic proteins from control and transgenic hearts with constitutively active or dominant negative PKCε were analyzed using difference in-gel electrophoresis (DIGE). Among the differentially expressed proteins were creatine kinase, pyruvate kinase, lactate dehydrogenase, and the cytosolic isoforms of aspartate amino transferase and malate dehydrogenase, the two enzymatic components of the malate aspartate shuttle, which are required for the import of reducing equivalents from glycolysis across the inner mitochondrial membrane. These enzymatic changes appeared to be dependent on PKCε activity, as they were not observed in mice expressing inactive PKCε. High-resolution proton nuclear magnetic resonance (^{1}H-NMR) spectroscopy confirmed a pronounced effect of PKCε activity on cardiac glucose and energy metabolism: normoxic hearts with constitutively active PKCε had significantly lower concentrations of glucose, lactate, glutamine and creatine, but higher levels of choline, glutamate and total adenosine nucleotides. Moreover, the depletion of cardiac energy metabolites was slower during ischemia/reperfusion injury and glucose metabolism recovered faster upon reperfusion in transgenic hearts with active PKCε. Notably, inhibition of PKCε resulted in compensatory phosphorylation and mitochondrial translocation of PKCδ. Taken together, our findings are the first evidence that PKCε activity modulates cardiac glucose metabolism and provide a possible explanation for the synergistic effect of PKCδ and PKCε in cardioprotection.

1. Introduction

Protein kinase C (PKC) is a heterogeneous family of phospholipid-dependent kinases. Notably, the PKCε and the PKCδ isoforms have both been implicated in cardioprotection as translocation of activated PKCε and PKCδ to the membrane fraction has been detected in preconditioned hearts [1]. PKCε activation and PKCδ inhibition are thought to be involved in myocardial salvage and combined treatment with PKCδ inhibitor and PKCε activator peptides exerted an additive protective effect on the ischemic heart [2–7]. On the other hand, expression of active PKCδ increased resistance to simulated ischemia in neonatal cardiomyocytes [8]. Thus, although it is now widely accepted that PKC isoforms play a pivotal role in mediating both the early and the late phase of ischemic preconditioning [9–11], the mechanisms responsible for PKC-mediated ischaemic preconditioning are still debated. While numerous studies have addressed potential targets of PKC in cardiac signalling [12–15], the role of these specific PKC isoforms in cardiac metabolism is less clear.

To further advance our understanding of how PKC isoforms alter cardiac metabolism, we have previously identified protein and metabolite changes after ischemic preconditioning [16] and demonstrated that loss of PKCδ altered glucose metabolism resulting in a reduction in the ratio of cardiac glucose to lipid metabolites [17]. We now integrate protein with metabolite changes in cardioprotected mice with transgenic activation of PKCε and unravel metabolic changes occurring during ischemia/reperfusion injury. Our data are the first evidence that the cardioprotective effect of PKCε activation on mitochondrial function may be, in part, an indirect effect of modulating cardiac glucose metabolism providing an explanation for the synergistic effects of PKCε and PKCδ in cardioprotection.

2. Methods

Detailed methodology is provided in the online data supplement.

* Corresponding author. Tel.: +44 0 20 7848 5238; fax: +44 0 20 7848 5296.
E-mail address: manuel.mayr@kcl.ac.uk (M. Mayr).

0022-2828/$ – see front matter © 2008 Elsevier Inc. All rights reserved.
doi:10.1016/j.yjmcc.2008.10.008

2.1. Transgenic mice

Animals used in the present study were PKCε transgenic mice (ICR background) generated using a cDNA of active PKCε driven by the α-myosin heavy chain promoter to achieve cardiac-specific expression [12,18]. AE PKCε transgenic mice express a PKCε molecule that favors the open and active conformation (A to E mutation at A159), whereas DN PKCε mice express a dominant negative form of the same molecule (A to E mutation at A159 and K to R mutation at K436). The hearts of AE PKCε mice exhibit a 6-fold overexpression of PKCε and an inherent resistance to infarction (as compared to wild type, ICR controls) that is not observed in the DN PKCε mice [12]. Transgenic and control mice were sacrificed at the age of 6 months. Only male animals were used in all the experiments. Hearts from 8-week-old PKCδ-deficient mice served as controls for validating the antibody specificity [19].

2.2. Subcellular fractionation

Isolation of mitochondria was performed in the cold room at 4 °C. Freshly-harvested mouse hearts were minced in 250 mM sucrose, 1 mM EGTA, 20 mM Hepes, pH 7.5 with a glass homogenizer. Nuclei and unbroken cells were pelleted by centrifugation at 1000 *g* for 10 min. The crude mitochondrial and cytosolic fraction was obtained from the supernatant by centrifugation at 4000 *g* for 30 min. The membrane fraction was obtained by centrifugation of the cytosolic fraction at 100,000 *g* for 1 h.

2.3. Proteomics

Key techniques involved adaptations of previously published protocols, including those for difference in-gel electrophoresis (DIGE) [20], and nano-liquid chromatography tandem mass spectrometry (nano-LC MS/MS) [21]. Methods are described online. A detailed methodology is also available on our website http://www.vascular-proteomics.com. For proteomic analysis, mitochondrial and cytosolic protein extracts were prepared from 16 murine hearts ($n=6$ for control and AE mice, $n=4$ for DN mice). Two samples were pooled for each gel to obtain sufficient material for proteomic analysis. Differences in protein expression were analyzed using the Decyder software (Version 6.5, GE healthcare).

2.4. Murine model of regional myocardial ischemic injury

Myocardial infarction was induced in the anesthetized mouse using an established protocol of regional ischemic injury [22]. Briefly, male ICR mice were subjected to a 30 min left anterior descending coronary artery occlusion followed by 30 min of reperfusion. Sham control group was subjected to open chest surgery without coronary occlusion.

2.5. Metabolomics

For metabolomic analysis, metabolite extracts were prepared from 29 murine hearts ($n=5$ for normoxic control and AE PKCε mice, $n=4$ for control and $n=3$ for AE PKCε mice after ischemia, and $n=4$ for control, AE and DN PKCε mice after 30 min reperfusion, respectively). Water-soluble metabolites were extracted in 6% perchloric acid and proton magnetic resonance spectroscopy (^{1}H-NMR) was performed as described online [23].

2.6. Statistical analysis

Statistical analysis was performed using the analysis of variance (ANOVA) and unpaired Student's *t*-test. Pairwise comparisons between metabolites were performed using the Bonferroni/Dunn

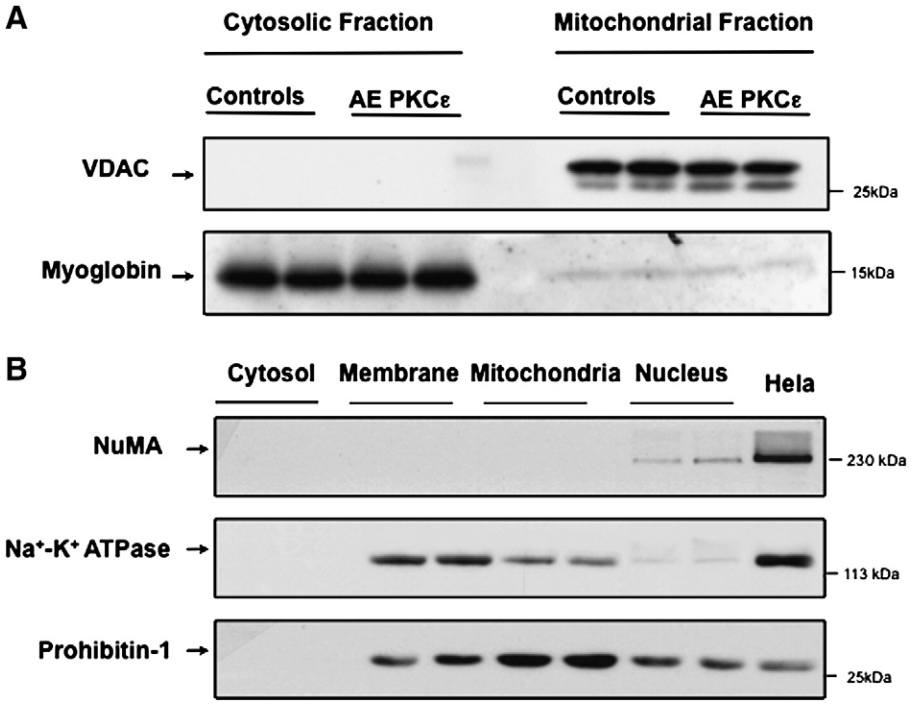

Fig. 1. Subcellular fractionation. Mitochondrial and cytosolic extracts were prepared from murine hearts as described in the Methods section. The purity of the fractions was assessed by Western blotting for VDAC, a mitochondrial outer membrane protein, and myoglobin, an abundant cytosolic protein (A). Panel B illustrates the depletion of nuclear proteins (NuMA) and the enrichment of mitochondrial (prohibitin) compared to other membrane proteins (Na^+/K^+ ATPase).

test. Results were given as means ± SE. A P value <0.05 was considered significant. Principal component analysis (PCA) was used for the analysis of the multivariate data produced by proteomic and metabolomic technologies, which reduces the data dimensionality. For proteomic datasets, DIGE gels were analyzed using the extended data analysis (EDA) module of the Decyder software (GE healthcare). For metabolite profiles, the ^{1}H-NMR spectra were used for generating bucket tables for PCA analysis.

3. Results

3.1. The proteome of PKCε transgenic hearts

To provide insights into potential cellular targets of PKCε, we compared the mitochondrial and cytosolic proteome of control hearts and transgenic hearts with constitutively active (AE) and dominant negative (DN) PKCε by DIGE. The quality of subcellular fractionation was assessed by immunoblotting (Fig. 1). The intactness of mitochondria was verified by the calcium swelling assay as described [24]. A representative image of the cardiac mitochondrial and cytosolic fraction as separated by two-dimensional gel electrophoresis (2-DE, pH 3–10 nonlinear) is presented in Fig. 2. Differentially expressed spots are numbered and protein identifications as obtained by nano-LC MS/MS analysis are listed in online Tables I–III. Only a few mitochondrial proteins in AE transgenic hearts were consistently different from control as well as DN transgenic hearts, including mitofilin (Supplemental Fig. 1A), an inner mitochondrial membrane protein and regulator of metabolic flux, and manganese superoxide dismutase, an important mitochondrial antioxidant (Supplemental Table I). The latter was subsequently confirmed by immunoblotting (Supplemental Fig. 2). No difference in net expression was observed for mitofillin because post-translational modifications as well as changes in net expression can be visualized on 2-DE gels (Supplemental Fig. 1A).

Besides mitochondria, several cytosolic enzymes related to glucose and energy metabolism were profoundly influenced by PKCε activation (Supplemental Table III, Supplemental Fig. 1B), including pyruvate kinase, enolase, lactate dehydrogenase, creatine kinase, as well as cytosolic malate dehydrogenase and cytosolic aspartate aminotransferase. The latter two enzymes constitute the components of the malate–aspartate shuttle, which exchanges cytoplasmic malate for mitochondrial aspartate and allows the transport of glycolytically-derived reducing equivalents across the inner mitochondrial membrane. When cross-validation was performed using principal component analysis (PCA) to investigate the global variation in the proteomic space, the differentially expressed cytosolic proteins allowed a clear separation of control and transgenic hearts (Figs. 3A–C).

Unexpectedly, the proteomic experiments also revealed a pronounced effect of PKCε inhibition on the mitochondrial pyruvate dehydrogenase complex (Supplemental Table II). The latter consists of E1 [the pyruvate dehydrogenase (decarboxylating) (alpha)2/(beta)2 heterotetramer], E2 (the dihydrolipoamide acetyltransferase) and E3 (the dihydrolipoyl dehydrogenase). Component X is an E3-binding protein and/or an E2 ancillary subunit with E2-like activity. Given that a 1:1 stoichiometry should exist between E1-alpha and E1-beta, the opposing directionality in changes observed in the proteomic experiment, suggests a post-translational modification. This was further substantiated by our finding that pyruvate dehydrogenase kinase 4, an inducible regulatory component, was identified within the protein spot containing E1-alpha. Phosphorylation of E1 by pyruvate dehydrogenase kinase (PDK) inactivates E1 and subsequently the entire pyruvate dehydrogenase complex. No statistically significant

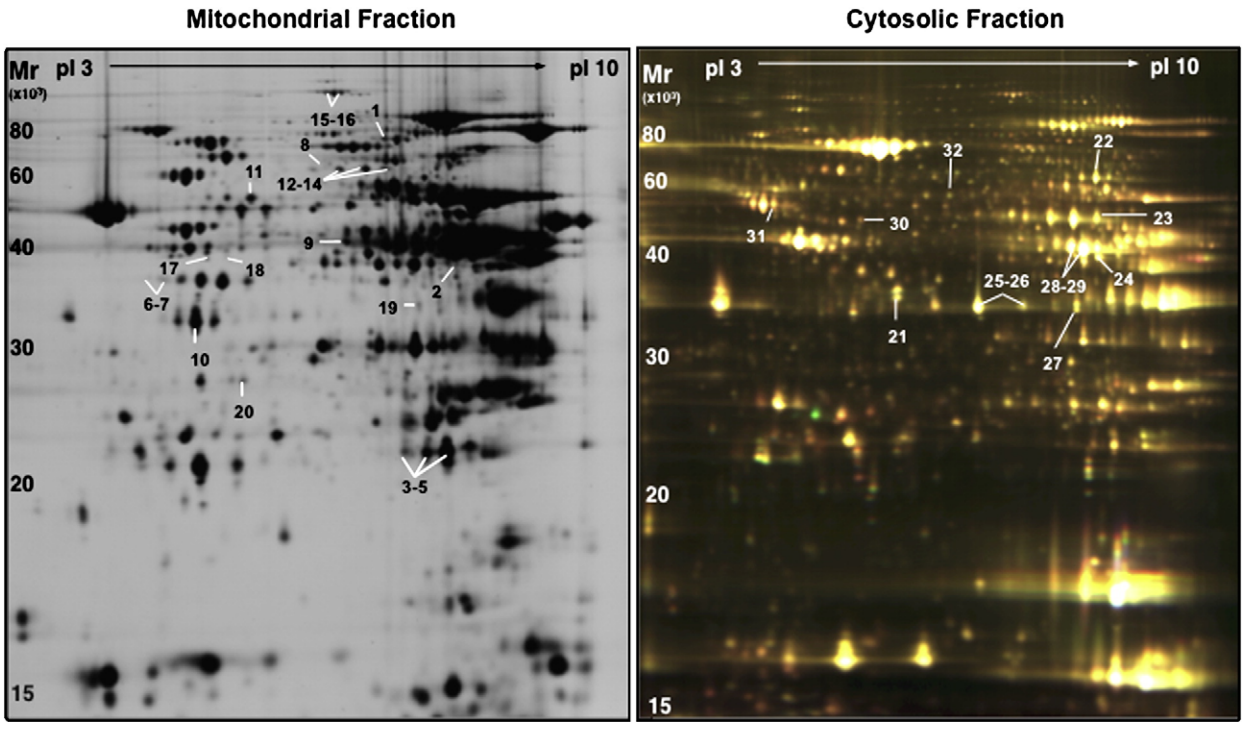

Fig. 2. 2-DE map of cardiac proteins in the mitochondrial and cytosolic fraction. Subcellular protein extracts were pre-labelled with Cy3 and Cy5 using the DIGE approach and co-separated on large format 2-DE gels using pH 3-10NL IPG strips followed by 12% SDS polyacrylamide gels. Images were acquired on a fluorescence scanner and counterstained with silver. A silver-stained image of mitochondrial extracts and a DIGE image of cytosolic extracts is shown in panels A and B, respectively. Analyses using DeCyder® software revealed the spots showing a significant difference in AE or DN hearts. Proteins were numbered and identified by nano-LC MS/MS (Supplemental Table I–III).

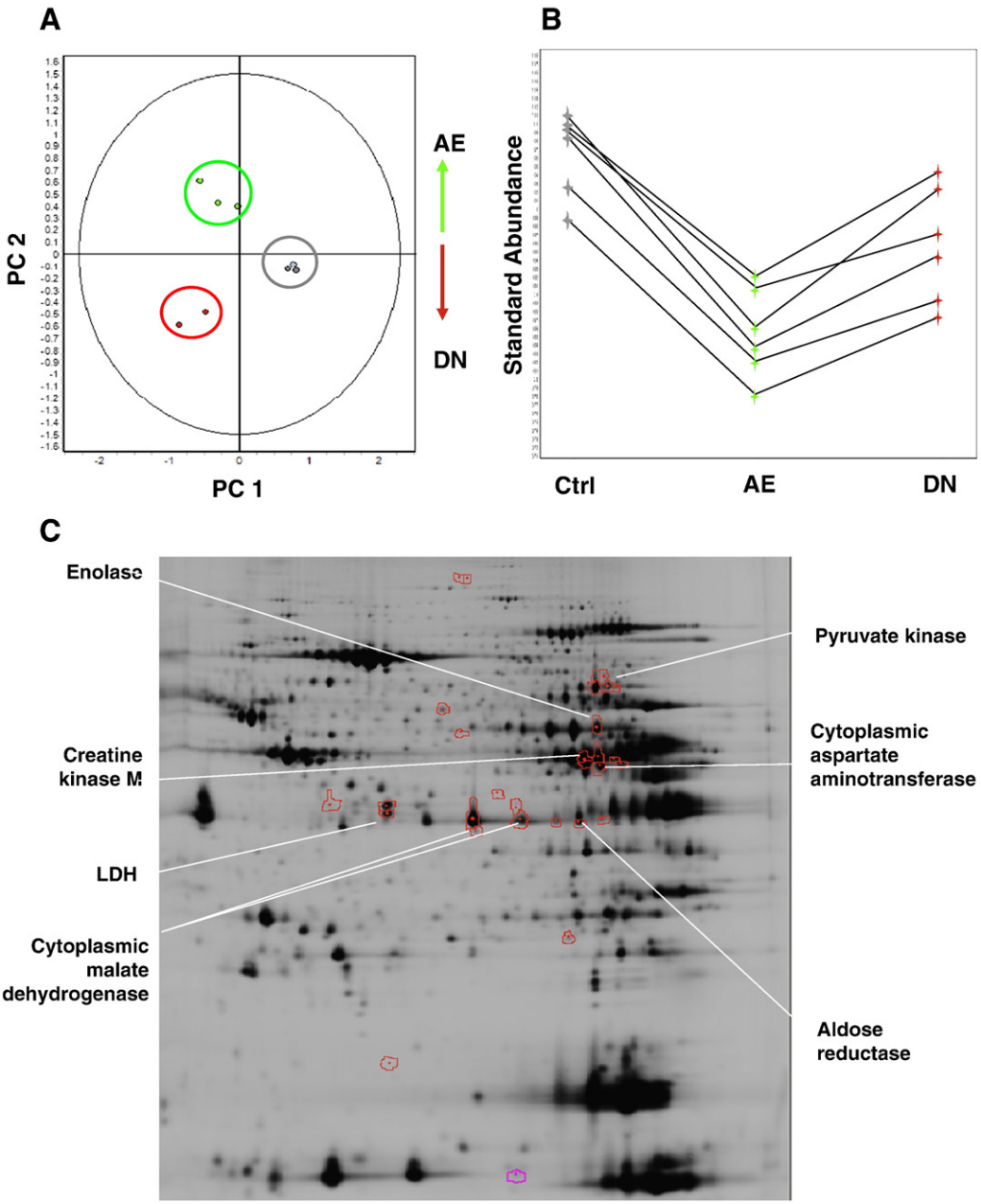

Fig. 3. Differential expression of cytosolic enzymes in PKCε transgenic hearts. Principal Component Analysis on the set of differentially expressed cytosolic proteins (ANOVA<0.05) allowed clear discrimination of controls (grey), AE (green) and DN PKCε hearts (red) (A). The differentially expressed enzymes contributing to this discrimination formed a cluster of similar expression profiles (B) and are highlighted on the representative 2-DE gel shown below (C).

differences were found for cytosolic proteins. When the differentially expressed proteins were submitted to Ingenuity Pathway Analysis (Ingenuity System, Mountain View, CA), the computational algorithms built two dominant protein association networks (Supplemental Fig. 3) and returned pyruvate metabolism as the top canonical pathway. Thus, our proteomic data provide strong evidence for a previously unrecognized effect of PKCε activity on cardiac glucose metabolism.

3.2. Metabolomic analysis of normoxic PKCε transgenic hearts

To prove the functional relevance of the described enzymatic changes, we applied high-resolution ^{1}H-NMR spectroscopy to measure cardiac metabolites. A representative ^{1}H-NMR spectrum of control and AE PKCε transgenic hearts is shown in Fig. 4. A principal component (PCA) and a linear discriminant analysis (LDA) were performed to investigate the global variation of the cardiac samples in the 25-dimensional metabolite space. AE PKCε and control hearts were dissimilar enough that principal component 1 (PC1) alone gave good discrimination (Supplemental Fig. 4A). 9/10 samples were correctly classified, with 1 control misclassified (LDA, leave one out). The scores on PC1 were −0.0565, −0.0039, −0.0420, −0.0321, 0.0015 for control and 0.0256, 0.0363, 0.0236, 0.0169, 0.0307 for AE PKCε hearts. The difference between the two means (blue) and PC1 (green) is plotted in the bottom panel of Fig. 4. The fact that the difference between the 2 means and the direction of largest variance (PC1) is so small suggests that the two groups are well separated, which is

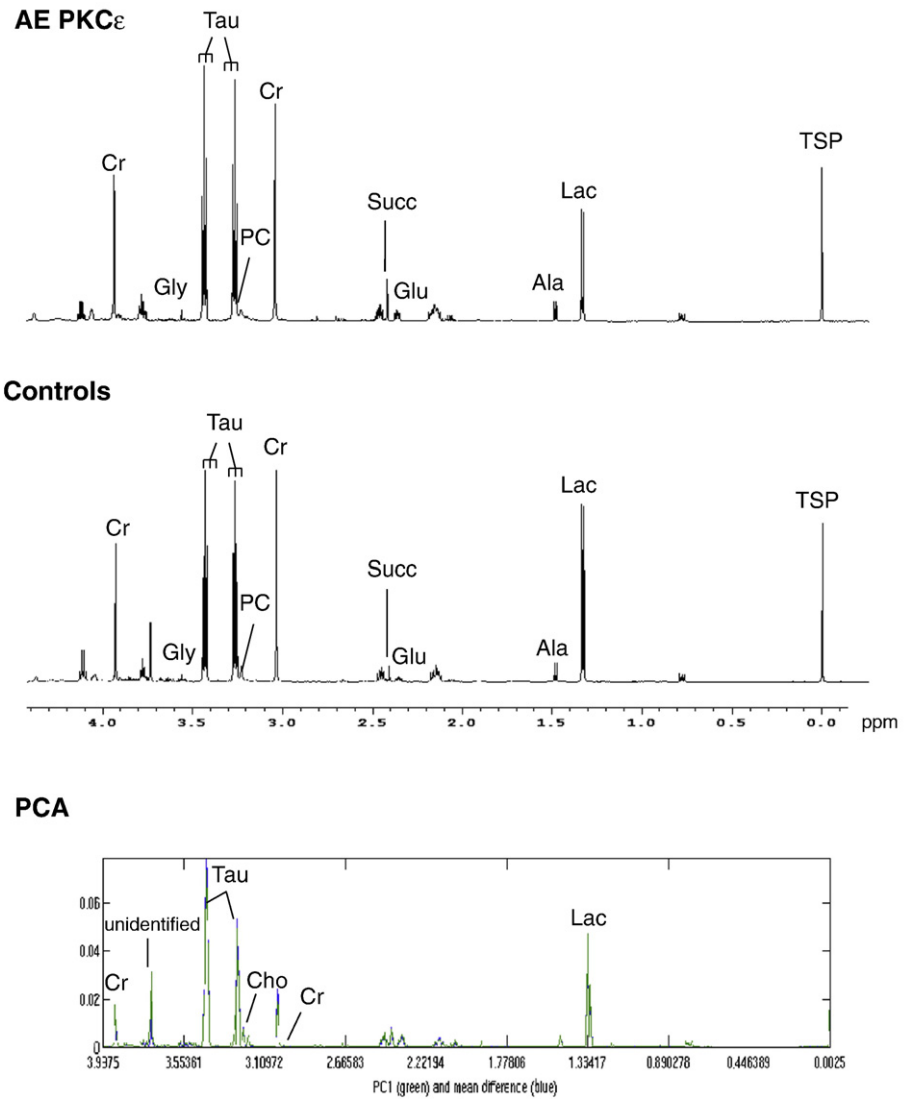

Fig. 4. Nuclear magnetic resonance spectra of murine hearts. Representative high-resolution ^{1}H-NMR spectra of AE PKCε transgenic and control hearts. Within the aliphatic region of the NMR spectra (−0.05 to 4.2 parts per million), resonances have been assigned to 25 metabolites, including creatine (Cr), glycine (Gly), taurine (Tau), phosphocholine (PC), succinate (Succ), glutamate (Glu), alanine (Ala), and lactate (Lac). Sodium 3-trimethylsilyl-2,2,3,3-tetradeuteropropionate (TSP) was added into the samples for chemical shift calibration. The bottom panel shows the first principal component (PC1) and the differences between the two means of metabolites in hearts with and without PKCε activation.

confirmed by the cross-validated classification. Metabolites responsible for the discrimination between the two groups have been assigned. The quantitative data are included as online Table IV. Levels of lactate, glucose, glutamine, leucine, taurine and total creatine were significantly lower in cardioprotected AE PKCε transgenic hearts, while choline, glutamate and adenosine nucleotides were higher compared to controls (Fig. 5A).

3.3. Metabolomic analysis after ischemia/reperfusion injury

To trace metabolite changes during ischemia/reperfusion injury, we measured cardiac metabolites after 30 min of ischemia and 30 min reperfusion. Strikingly, no significant metabolite changes were detected between control and AE PKCε transgenic hearts immediately after ischemia (Supplemental Table V), but differences reappeared upon reperfusion (Supplemental Table VI, Supplemental Fig. 4B): After only 30 min of reperfusion, the adenosine nucleotide pool was again significantly higher in AE PKCε transgenic hearts. Similarly, the decline of the total creatine pool during ischemia/reperfusion injury was less pronounced. This maintenance of cardiac energy metabolites in AE PKCε transgenic hearts coincided with a faster recovery of glucose metabolites (Fig. 5B). A direct comparison of average metabolite concentrations in control, AE and DN PKCε transgenic hearts provides further evidence that the activity of PKCε correlates with metabolic recovery upon reperfusion (Fig. 6).

3.4. Mitochondrial translocation of PKCδ in PKCε transgenic hearts

While cardiac glucose metabolism was clearly affected by PKCε activity, it remained to be determined whether there was a cross-talk between the PKCε and the PKCδ isoform [25]. Fig. 7 provides evidence that activation of PKCε did not lead to a compensatory change in PKCδ expression. Inhibition of PKCε, however, markedly increased phosphorylation of PKCδ at Thr^{505} and promoted translocation of PKCδ to the cardiac mitochondria (Fig. 7A). The specificity of the antibodies was confirmed by using PKCδ-deficient hearts (Figs. 7B, C). These

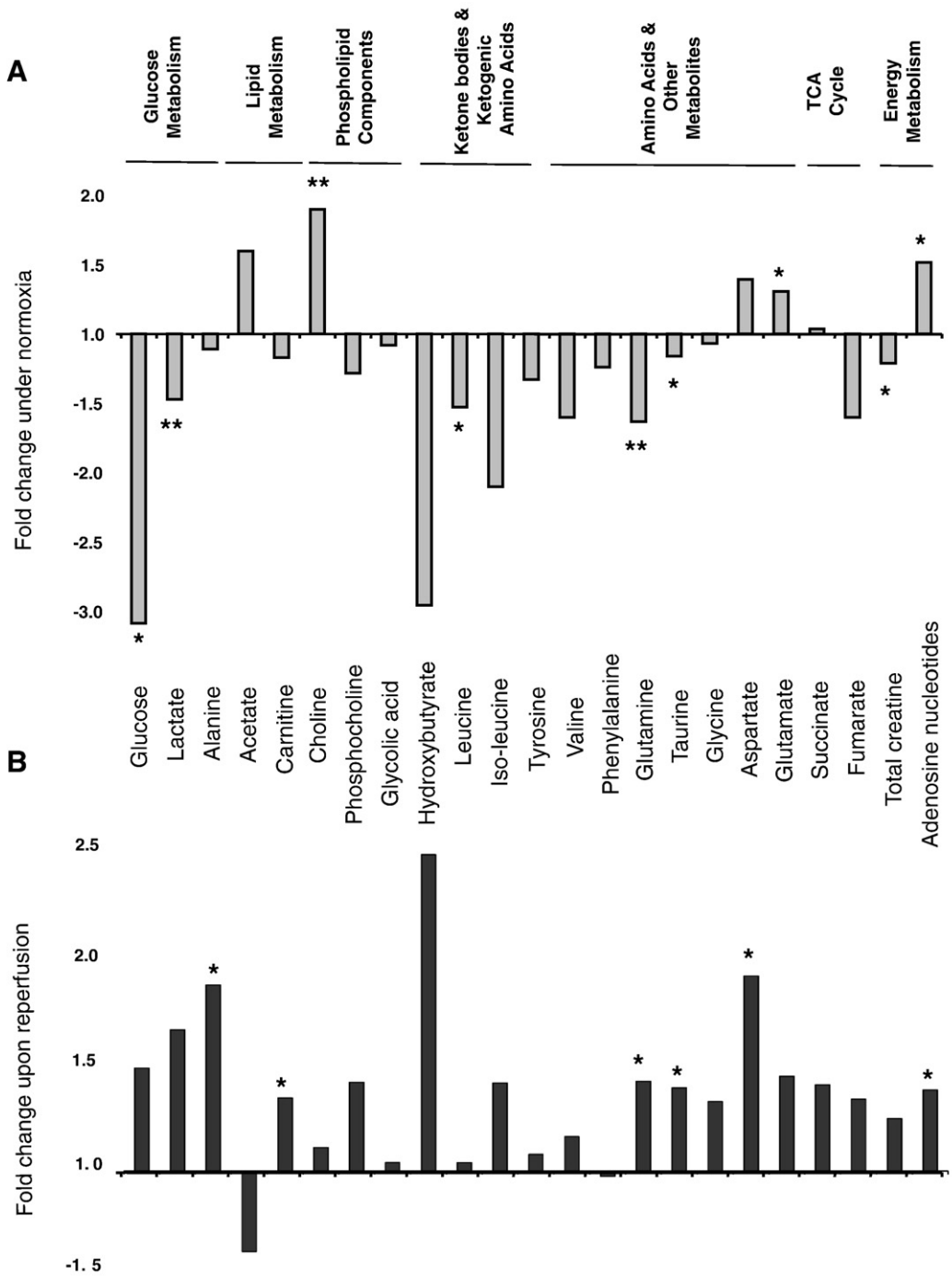

Fig. 5. Comparison of metabolites during normoxia (A) and after ischemia/reperfusion injury (B). The histogram shows the fold change of metabolites in AE PKCε hearts normalized to controls. Note the inverse pattern of most cardiac metabolites before (A) and after ischemia/reperfusion injury (B), but the consistent elevation of the adenosine nucleotide pool in AE PKCε hearts. * Significant difference $p<0.05$, ** $p<0.01$

results provide additional support for the differential expression of the pyruvate dehydrogenase complex in DN PKCε hearts (Supplemental Table II), as PKCδ Thr^{505} phosphorylation is known to alter substrate specificity [26] and the pyruvate dehydrogenase complex is one of the likely targets of PKCδ on cardiac mitochondria [16,17,27]. Thus, the activation state of PKCε influences PKCδ and the pyruvate dehydrogenase complex, the key enzyme linking glycolysis to mitochondrial respiration.

4. Discussion

In previous studies, our laboratory has shown that transgenic activation of PKCε in the heart is sufficient to significantly reduce myocardial infarction after coronary artery occlusion [12,28]. In the present study, we used a novel combination of gel-based proteomics and high-resolution ^{1}H-NMR spectroscopy-based metabolomics [29], to investigate mechanisms of PKCε-mediated cardioprotection. This

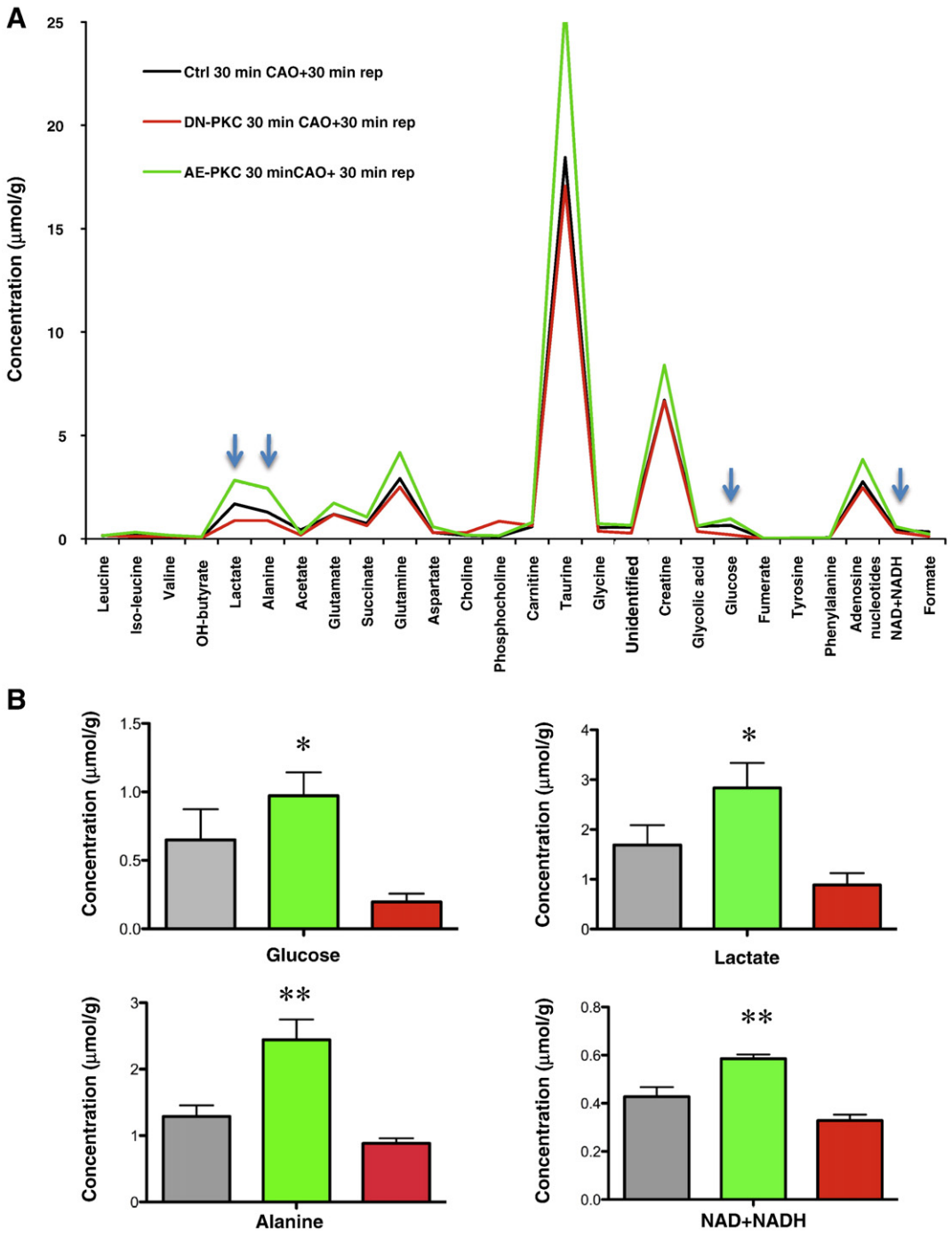

Fig. 6. Metabolic recovery after ischemia/reperfusion. Average metabolite concentration after 30 min of reperfusion in control, AE and DN transgenic hearts (A). The short reperfusion time was adapted to assess the early recovery of cardiac metabolism upon restoration of blood flow. Note that concentrations of metabolites related to glucose metabolism (arrows) correlate with PKCε activity (B). * Statistically significant difference from DN hearts, ** statistically significant difference from control as well as DN hearts.

comprehensive analysis revealed that PKCε activation has a previously unrecognized effect on cardiac glucose metabolism [30,31].

4.1. PKCε and cardiac metabolism

Despite abundant information on PKCε signalling networks in the heart [12–14,32], the manner in which the actions of these various signalling molecules integrate into cardiac metabolism is still not well understood. To our knowledge, only two papers have previously addressed the effects of PKCε activation on cardiac metabolism: Cross et al [33] used ^{31}P-NMR spectroscopy to measure phosphorus metabolites during ischemia reperfusion injury in Langendorff-perfused hearts. Despite maintaining a greater level of myocardial ATP during ischemia and reperfusion, the phosphocreatine content in AE PKCε transgenic hearts was similar to controls. McCarthy [34] et al. subsequently evaluated this phenotype in isolated mitochondria: they described a modest basal hyperpolarization in mitochondria from AE PKCε transgenic hearts *versus* controls. While no difference was

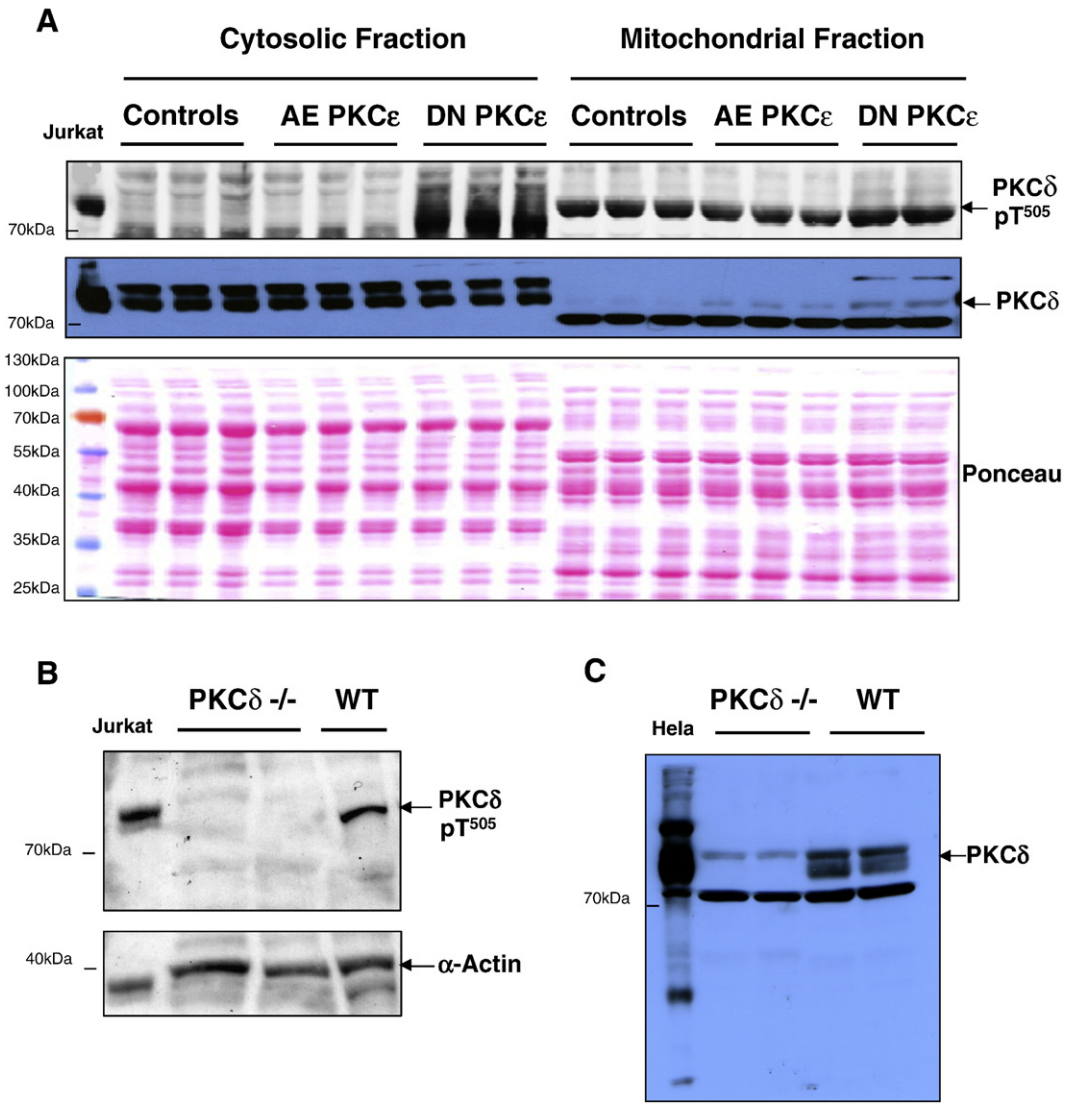

Fig. 7. Mitochondrial translocation of PKCδ. Mitochondrial extracts of control, AE and DN PKCε hearts were analyzed by Western blotting and probed with antibodies for phospho-PKCδ (Thr^{505}) and total PKCδ. Ponceau red staining served as a loading control. Note the increase in phosphorylation and mitochondrial translocation of PKCδ upon inactivation of PKCε. pT denotes phosphothreonine (A). Verification of the antibody specificity by using hearts from PKCδ-deficient mice (B, C). The antibody for PKCδ-pThr^{505} showed good specificity. The antibody for total PKCδ recognizes three bands, of which the middle one is specific for PKCδ.

observed in basal mitochondrial respiratory function by measuring oxygen consumption, respiratory-control index, and the rate of ATP production, PKCε activation augmented mitochondrial respiratory capacity in response to anoxia–reoxygenation. However, many issues of metabolism in AE PKCε hearts remain unresolved, especially with respect to the hearts *in vivo*.

4.2. Proteomics and metabolomics combined

Previous proteomic analyses of cardiac PKCε signalling complexes revealed metabolic enzymes as potential interacting partners of this serine/threonine kinase [13,32]. We now demonstrate that some of the previously identified PKCε targets, i.e. creatine kinase, enolase, and the mitochondrial malate carrier, are indeed among the differentially expressed proteins in AE PKCε transgenic hearts. Moreover, as no data were available on how these interactions between PKCε and metabolic enzymes influence cardiac metabolism, we quantified cardiac metabolites in control and transgenic hearts under normoxia, after ischemia and after reperfusion injury. Our ^{1}H-NMR data on extracted cardiac metabolites not only confirmed the ^{31}P-NMR data on Langendorff-perfused hearts [33] in that cardiac energy metabolites were better preserved in AE PKCε transgenic hearts, but also provide a mechanistic underpinning for the observed cardioprotective phenotype: activation of PKCε resulted in lower lactate levels and a similar downregulation of cytosolic malate dehydrogenase isoforms as previously observed in preconditioned wildtype hearts [16]. Thus, PKCε activation induces proteomic and metabolic characteristics of a preconditioned cardiac phenotype, which were previously found to be abolished in hearts with targeted disruption of the PKCδ gene [16].

4.3. Cross-talk between PKCε and PKCδ

The striking consistency between different genetically engineered mouse models suggests that the metabolic effects of PKCε may, at least partially, be interrelated with PKCδ. Subsequent experiments

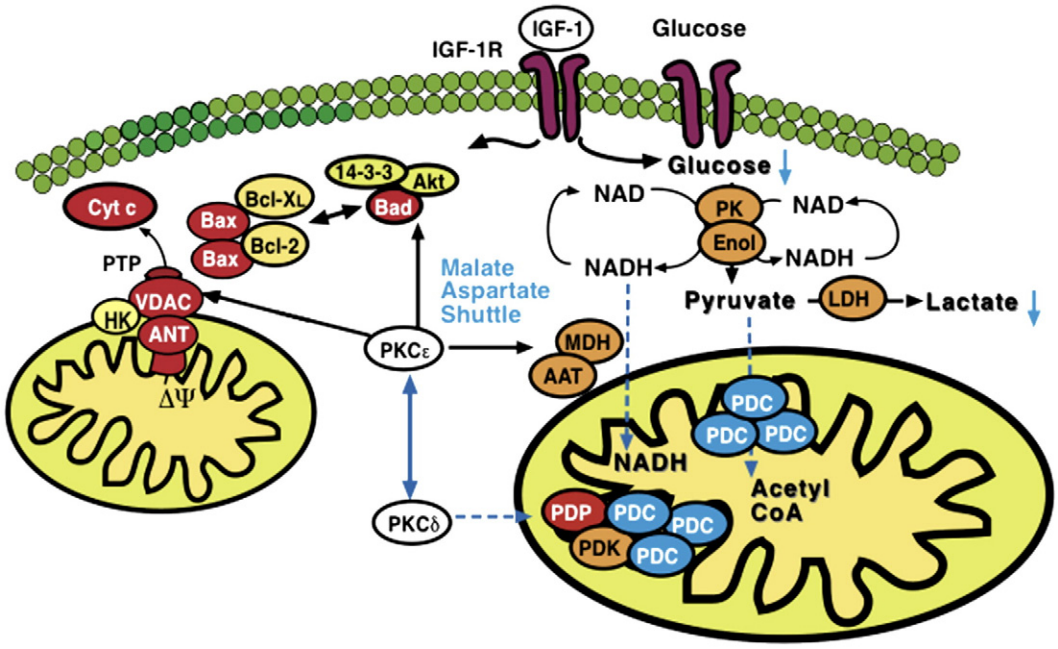

Fig. 8. Model for PKCε-initiated metabolic changes linked to cardioprotection. PKCε activation resulted in differential expression of pyruvate kinase (PK), enolase (Enol) and lactate dehydrogenase (LDH) with a corresponding reduction of glucose and lactate in murine hearts. Notably, a pronounced effect was also observed on cytosolic malate dehydrogenase (MDH) and aspartate aminotransferase (AAT), the two enzymatic components of the malate–aspartate shuttle. The latter transfers electrons from the cytoplasm to mitochondria and is important in allowing maximum release of the free energy in glycolysis under aerobic conditions. In contrast, inhibition of PKCε stimulated loop phosphorylation and translocation of PKCδ to cardiac mitochondria, where it targets the pyruvate dehydrogenase complex (PDC), the enzyme responsible for converting the glycolytic endproduct pyruvate to acetyl-CoA. The pyruvate dehydrogenase complex is located at the inner mitochondrial membrane and inhibited when phosphorylated by pyruvate dehydrogenase kinase (PDK) and activated upon dephosphorylation by pyruvate dehydrogenase phosphatase (PDP). Thus, PKCε and PKCδ activities influence key enzymatic reactions bridging aerobic and anaerobic glucose metabolism.

confirmed a pronounced effect of PKCε activity on PKCδ translocation to cardiac mitochondria. Previously, increased expression and activation of PKCδ was observed in *PKCε*−/− mice [35,36]. However, increased PKCδ activity in the complete absence of PKCε did not result in mitochondrial translocation of the PKCδ isoform. In our study, cardiac-specific manipulation of PKCε activity did not alter PKCδ expression, but inhibition of PKCε was associated with increased PKCδ loop phosphorylation, mitochondrial translocation and differential expression of the pyruvate dehydrogenase complex. These data confirm our previous results in PKCδ-deficient mice, where altered activity of the pyruvate dehydrogenase complex was postulated to be a likely explanation for the observed metabolic effects after deletion of the PKCδ gene [16,17,37].

Notably, despite increased PKCδ on mitochondria, transgenic hearts with DN PKCε showed no cardioprotective phenotype, which may be consistent with previous reports claiming that translocation of PKCδ is required for mediating cardioprotection after pharmacological [38], but not ischemic preconditioning [39]. On the other hand, a moderate increase in mitochondrial PKCδ was also observed in AE PKCε hearts and similar to mice deficient for PKCε [35], PKCδ knockout mice lost cardioprotection in response to ischemic preconditioning [16]. In fact, cardiac damage was even exaggerated by ischemic preconditioning in the absence of PKCδ [16]. This finding is in line with a recent clinical trial [40], demonstrating that the intra-coronary application of high doses of a PKCδ inhibitor during primary percutaneous coronary intervention was associated with an increase, rather than a decrease, in infarct size [41]. Thus, deficiency for either PKCε or PKCδ is sufficient to abrogate the cardioprotective effects of ischemic preconditioning, indicating that an individual PKC isoform may not be cardioprotective *per se*, but that cardioprotection may require the interaction of both PKC isoforms and that the cardioprotective effect may be the consequence of their combined orchestration of cardiac glucose and energy metabolism (Fig. 8).

4.4. Limitations of the study

Although proteomics and metabolomics offer a suite of tools to interrogate tissue metabolism [29,37,42], it is important to acknowledge that both techniques are biased to high-abundant components. Moreover, metabolites were extracted directly from snap-frozen hearts and a reduction of a metabolite as measured by ^{1}H-NMR spectroscopy may be the consequence of increased consumption or decreased production. As enzymatic activity in tissues is reflected in the expression and post-translational modifications of enzymes [43], 2-DE offers a particular advantage by visualizing posttranslational modifications of high abundant enzymes as a shift in isoelectric point or molecular weight [44]. In combination, these emerging technologies contribute to a better understanding of enzymatic and metabolite changes associated with PKCε-mediated cardioprotection.

4.5. Conclusion

While activation of PKCε and inhibition of PKCδ were known to be cardioprotective against ischemia/reperfusion injury, the common denominator in cardioprotective signalling between the two PKC isoforms remained unknown. Our studies demonstrate that PKCε and PKCδ influence key steps in glucose metabolism of murine hearts. Thus, these kinases appear to be uniquely positioned to integrate signalling with metabolism, a central determinant of cardiomyocyte life and death. Future studies will have to address whether a similar interplay between the two PKC isoforms is also observed in human hearts and other experimental models of cardioprotection.

Acknowledgments

This work emanates from the European Vascular Genomics Network (http://www.evgn.org), a Network of Excellence supported by the European Community's sixth Framework Programme for Research Priority 1 "Life sciences, genomics and biotechnology for health" (Contract No. LSHM-CT-2003-503254). This work was supported in part by grants from the British Heart Foundation to M. Mayr and Q. Xu, by the Oak Foundation to Q. Xu, by NIH grants HL-76526, HL63901, HL65431, HL 80691, and HL-80111 to P. Ping, and Laubisch Endowment to P Ping. M. Mayr is supported by a Senior Research Fellowship of the British Heart Foundation.

Appendix A. Supplementary data

Supplementary data associated with this article can be found, in the online version, at doi:10.1016/j.yjmcc.2008.10.008.

References

[1] Mackay K, Mochly-Rosen D. Localization, anchoring, and functions of protein kinase C isozymes in the heart. J Mol Cell Cardiol 2001;33(7):1301–7.
[2] Hahn HS, Yussman MG, Toyokawa T, Marreez Y, Barrett TJ, Hilty KC, et al. Ischemic protection and myofibrillar cardiomyopathy: dose-dependent effects of in vivo deltaPKC inhibition. Circ Res 2002;91(8):741–8.
[3] Chen L, Hahn H, Wu G, Chen CH, Liron T, Schechtman D, et al. Opposing cardioprotective actions and parallel hypertrophic effects of delta PKC and epsilon PKC. Proc Natl Acad Sci U S A 2001;98(20):11114–9.
[4] Inagaki K, Hahn HS, Dorn 2nd GW, Mochly-Rosen D. Additive protection of the ischemic heart ex vivo by combined treatment with {delta}-protein kinase C inhibitor and {epsilon}-protein kinase C activator. Circulation 2003.
[5] Murriel CL, Churchill E, Inagaki K, Szweda LI, Mochly-Rosen D. Protein kinase C {delta} activation induces apoptosis in response to cardiac ischemia and reperfusion damage: a mechanism involving BAD and the mitochondria. J Biol Chem 2004;279(46):47985–91.
[6] Dorn 2nd GW, Souroujon MC, Liron T, Chen CH, Gray MO, Zhou HZ, et al. Sustained in vivo cardiac protection by a rationally designed peptide that causes epsilon protein kinase C translocation. Proc Natl Acad Sci U S A 1999;96(22):12798–803.
[7] Liu GS, Cohen MV, Mochly-Rosen D, Downey JM. Protein kinase C-epsilon is responsible for the protection of preconditioning in rabbit cardiomyocytes. J Mol Cell Cardiol 1999;31(10):1937–48.
[8] Zhao J, Renner O, Wightman L, Sugden PH, Stewart L, Miller AD, et al. The expression of constitutively active isotypes of protein kinase C to investigate preconditioning. J Biol Chem 1998;273(36):23072–9.
[9] Bolli R. The late phase of preconditioning. Circ Res 2000;87(11):972–83.
[10] Kloner RA, Jennings RB. Consequences of brief ischemia: stunning, preconditioning, and their clinical implications: part 1. Circulation 2001;104(24):2981–9.
[11] Kloner RA, Jennings RB. Consequences of brief ischemia: stunning, preconditioning, and their clinical implications: part 2. Circulation 2001;104(25):3158–67.
[12] Ping P, Song C, Zhang J, Guo Y, Cao X, Li RC, et al. Formation of protein kinase C (epsilon)-Lck signaling modules confers cardioprotection. J Clin Invest 2002;109 (4):499–507.
[13] Ping P, Zhang J, Pierce Jr WM, Bolli R. Functional proteomic analysis of protein kinase C epsilon signaling complexes in the normal heart and during cardioprotection. Circ Res 2001;88(1):59–62.
[14] Baines CP, Zhang J, Wang GW, Zheng YT, Xiu JX, Cardwell EM, et al. Mitochondrial PKCepsilon and MAPK form signaling modules in the murine heart: enhanced mitochondrial PKCepsilon-MAPK interactions and differential MAPK activation in PKCepsilon-induced cardioprotection. Circ Res 2002;90(4):390–7.
[15] Zhang J, Baines CP, Zong C, Cardwell EM, Wang G, Vondriska TM, et al. Functional proteomic analysis of a three-tier PKCepsilon-Akt-eNOS signaling module in cardiac protection. Am J Physiol Heart Circ Physiol 2005;288(2):H954–61.
[16] Mayr M, Metzler B, Chung YL, McGregor E, Mayr U, Troy H, et al. Ischemic preconditioning exaggerates cardiac damage in PKC-{delta} null mice. Am J Physiol Heart Circ Physiol 2004;287(2):H946–56.
[17] Mayr M, Chung YL, Mayr U, McGregor E, Troy H, Baier G, et al. Loss of PKC-{delta} alters cardiac metabolism. Am J Physiol Heart Circ Physiol 2004;287(2):H937–45.
[18] Pass JM, Zheng Y, Wead WB, Zhang J, Li RC, Bolli R, et al. PKCepsilon activation induces dichotomous cardiac phenotypes and modulates PKCepsilon–RACK interactions and RACK expression. Am J Physiol Heart Circ Physiol 2001;280(3):H946–55.
[19] Leitges M, Mayr M, Braun U, Mayr U, Li C, Pfister G, et al. Exacerbated vein graft arteriosclerosis in protein kinase Cdelta-null mice. J Clin Invest 2001;108 (10):1505–12.
[20] Mayr M, Zampetaki A, Sidibe A, Mayr U, Yin X, De Souza AI, et al. Proteomic and metabolomic analysis of smooth muscle cells derived from the arterial media and adventitial progenitors of apolipoprotein E-deficient mice. Circ Res 2008;102(9): 1046–56.
[21] Gomes AV, Zong C, Edmondson RD, Li X, Stefani E, Zhang J, et al. Mapping the murine cardiac 26S proteasome complexes. Circ Res 2006;99(4):362–71.
[22] Wang G, Liem DA, Vondriska TM, Honda HM, Korge P, Pantaleon DM, et al. Nitric oxide donors protect murine myocardium against infarction via modulation of mitochondrial permeability transition. Am J Physiol Heart Circ Physiol 2005;288 (3):H1290–5.
[23] Mayr M, Yusuf S, Weir G, Chung YL, Mayr U, Yin X, et al. Combined metabolomic and proteomic analysis of human atrial fibrillation. J Am Coll Cardiol 2008;51 (5):585–94.
[24] Baines CP, Song CX, Zheng YT, Wang GW, Zhang J, Wang OL, et al. Protein kinase Cepsilon interacts with and inhibits the permeability transition pore in cardiac mitochondria. Circ Res 2003;92(8):873–80.
[25] Rybin VO, Guo J, Gertsberg Z, Elouardighi H, Steinberg SF. Protein kinase Cepsilon (PKCepsilon) and Src control PKCdelta activation loop phosphorylation in cardiomyocytes. J Biol Chem 2007;282(32):23631–8.
[26] Liu Y, Belkina NV, Graham C, Shaw S. Independence of protein kinase C-delta activity from activation loop phosphorylation: structural basis and altered functions in cells. J Biol Chem 2006;281(17):12102–11.
[27] Churchill EN, Murriel CL, Chen CH, Mochly-Rosen D, Szweda LI. Reperfusion-induced translocation of deltaPKC to cardiac mitochondria prevents pyruvate dehydrogenase reactivation. Circ Res 2005;97(1):78–85.
[28] Ping P, Zhang J, Qiu Y, Tang XL, Manchikalapudi S, Cao X, et al. Ischemic preconditioning induces selective translocation of protein kinase C isoforms epsilon and eta in the heart of conscious rabbits without subcellular redistribution of total protein kinase C activity. Circ Res 1997;81(3):404–14.
[29] Mayr M, Madhu B, Xu Q. Proteomics and metabolomics combined in cardiovascular research. Trends Cardiovasc Med 2007;17(2):43–8.
[30] Depre C, Vanoverschelde JL, Taegtmeyer H. Glucose for the heart. Circulation 1999;99(4):578–88.
[31] Vogt AM, Poolman M, Ackermann C, Yildiz M, Schoels W, Fell DA, et al. Regulation of glycolytic flux in ischemic preconditioning. A study employing metabolic control analysis. J Biol Chem 2002;277(27):24411–9.
[32] Edmondson RD, Vondriska TM, Biederman KJ, Zhang J, Jones RC, Zheng Y, et al. Protein kinase C epsilon signaling complexes include metabolism- and transcription/translation-related proteins: complimentary separation techniques with LC/MS/MS. Mol Cell Proteomics 2002;1(6):421–33.
[33] Cross HR, Murphy E, Bolli R, Ping P, Steenbergen C. Expression of activated PKC epsilon (PKC epsilon) protects the ischemic heart, without attenuating ischemic H (+) production. J Mol Cell Cardiol 2002;34(3):361–7.
[34] McCarthy J, McLeod CJ, Minners J, Essop MF, Ping P, Sack MN. PKCepsilon activation augments cardiac mitochondrial respiratory post-anoxic reserve—a putative mechanism in PKCepsilon cardioprotection. J Mol Cell Cardiol 2005;38(4): 697–700.
[35] Gray MO, Zhou HZ, Schafhalter-Zoppoth I, Zhu P, Mochly-Rosen D, Messing RO. Preservation of base-line hemodynamic function and loss of inducible cardioprotection in adult mice lacking protein kinase C epsilon. J Biol Chem 2004;279(5): 3596–604.
[36] Klein G, Schaefer A, Hilfiker-Kleiner D, Oppermann D, Shukla P, Quint A, et al. Increased collagen deposition and diastolic dysfunction but preserved myocardial hypertrophy after pressure overload in mice lacking PKCepsilon. Circ Res 2005;96 (7):748–55.
[37] Mayr M, Siow R, Chung YL, Mayr U, Griffiths JR, Xu Q. Proteomic and metabolomic analysis of vascular smooth muscle cells: role of PKCdelta. Circ Res 2004;94(10): e87–96.
[38] Fryer RM, Wang Y, Hsu AK, Gross GJ. Essential activation of PKC-delta in opioid-initiated cardioprotection. Am J Physiol Heart Circ Physiol 2001;280(3):H1346–53.
[39] Fryer RM, Hsu AK, Wang Y, Henry M, Eells J, Gross GJ. PKC-delta inhibition does not block preconditioning-induced preservation in mitochondrial ATP synthesis and infarct size reduction in rats. Basic Res Cardiol 2002;97(1):47–54.
[40] Bates E, Bode C, Costa M, Gibson CM, Granger C, Green C, et al. Intracoronary KAI-9803 as an adjunct to primary percutaneous coronary intervention for acute ST-segment elevation myocardial infarction. Circulation 2008;117(7):886–96.
[41] Metzler B, Xu Q, Mayr M. Letter by Metzler et al regarding article, "Intracoronary KAI-9803 as an adjunct to primary coronary intervention for acute ST-segment elevation myocardial infarction". Circulation 2008;118(4):e80.
[42] Mayr M, Chung YL, Mayr U, Yin X, Ly L, Troy H, et al. Proteomic and metabolomic analyses of atherosclerotic vessels from apolipoprotein E-deficient mice reveal alterations in inflammation, oxidative stress, and energy metabolism. Arterioscler Thromb Vasc Biol 2005;25(10):2135–42.
[43] Sun J, Morgan M, Shen RF, Steenbergen C, Murphy E. Preconditioning results in S-nitrosylation of proteins involved in regulation of mitochondrial energetics and calcium transport. Circ Res 2007;101(11):1155–63.
[44] Mayr M, Mayr U, Chung YL, Yin X, Griffiths JR, Xu Q. Vascular proteomics: linking proteomic and metabolomic changes. Proteomics 2004;4(12):3751–61.

PROTEOMIC AND METABOLOMIC ANALYSIS OF CARDIOPROTECTION: INTERPLAY BETWEEN PROTEIN KINASE C EPSILON AND DELTA IN REGULATING CARDIAC GLUCOSE METABOLISM OF MURINE HEARTS

Manuel Mayr, David Liem, Jun Zhang, Xiaohai Li, Nuraly K. Avliyakulov, Jeong In Yang, Glen Young, Tom M Vondriska, Christophe Ladroue, Basetti Madhu, John R. Griffiths, Aldrin Gomes, Qingbo Xu, Peipei Ping

Cardiovascular Division (MM, QX) King's College, University of London, UK; Cancer Research UK Cambridge Research Institute, Cambridge, UK, (BM, JRG); University of Warwick, UK (CL) and Department of Physiology (DL, JZ, XL, NA, JIY, GY, TMV, AG, PP) David Geffen School of Medicine, UCLA, Los Angeles, US

ONLINE DATA SUPPLEMENT

Correspondence to:

Dr. Manuel Mayr, Cardiovascular Division, King's College London School of Medicine, King's College London, 125 Coldharbour Lane, London SE5 9NU, UK

Phone: +44 (0) 20 7848 5238, Fax: +44 (0) 20 7848 5296

Email: manuel.mayr@kcl.ac.uk

ONLINE METHODS

Difference in-gel electrophoresis (DIGE). Mitochondrial pellets were resuspended in a standard lysis bufffer (9M urea, 1% DTT, 4% CHAPS, 0.8% Pharmalytes 3-10, protease and phosphatase inhibitors (Complete Mini, Roche). After centrifugation at 13,000 g for 10 min, the supernatant containing soluble proteins was harvested and the protein concentration was determined using a modification of the method described by Bradford [1]. Solubilised samples were divided into aliquots and stored at –80°C. For DIGE, proteins were precipitated (ReadyPrep 2-D Clean-up kit, Biorad) and resuspended in DIGE buffer (30mM TrisCl pH 8.5, 8M urea, 4% w/v CHAPS). The fluorescence dye labelling reaction was carried out at a dye/protein ratio of 400 pmol/100μg. After incubation on ice for 30 min, the labelling reaction was stopped by scavenging non-bound dyes with 10mM lysine for 15 min. For two-dimensional gel electrophoresis, extracts were loaded on nonlinear immobilized pH gradient 18-cm strips, 3-10 (GE healthcare). 100 μg per sample was applied to the IPG strip using an in-gel rehydration method. Samples were diluted in rehydration solution (8 M urea, 0.5% w/v CHAPS, 0.2% w/v DTT, and 0.2 % w/v Pharmalyte pH 3-10) and rehydrated overnight in a reswelling tray. Strips were focused at 0.05 mA/IPG strip for 35 kVh at 20°C (IPGphor, GE healthcare). Once IEF was completed the strips were equilibrated in 6M urea containing 30% v/v glycerol, 2% w/v SDS and 0.01% w/v Bromphenol blue, with addition of 1% w/v DTT for 15 min, followed by the same buffer without DTT, but with the addition of 4.8% w/v iodoacetamide for 15 min. SDS-PAGE was performed using 12% T (total acrylamide concentration), 2.6% C (degree of cross-linking) polyacrylamide gels without a stacking gel, using the Ettan DALT system (GE healthcare). The second dimension was terminated when the Bromphenol dye front had migrated off the lower end to the gels. After electrophoresis, fluorescence images were acquired using the Typhoon variable mode imager 9400 (GE healthcare). Finally, gels were fixed overnight in methanol: acetic acid: water solution (4:1:5 v/v/v). Protein profiles were visualised by silver staining

using the Plus one silver staining kit (GE healthcare) with slight modifications to ensure compatibility with subsequent mass spectrometry analysis [2]. For documentation, silver-stained gels were scanned in transmission scan mode using a calibrated scanner (GS-800, Biorad).

Nano-LC MS/MS. Gel pieces containing selected protein spots were treated overnight with modified trypsin (Promega) according to a published protocol modified for use with an Investigator ProGest (Genomic Solutions, Huntington, UK) robotic digestion system. Following enzymatic degradation, peptides were separated by a Surveyor HPLC system on a reverse-phase column and applied online to a LTQ ion-trap mass spectrometer. Spectra were collected from the ion-trap mass analyzer using full ion scan mode over the mass-to-charge (m/z) range 300-2000. MS-MS scans were performed on each ion using dynamic exclusion. Database search was performed using the TurboSEQUEST software (Thermo Finnigan). One missed cleavage per peptide was allowed and carbamidomethylation of cysteine as well as partial oxidation of methionine were assumed. The following filters were applied: Xcorr values of >2.0 (+1 charge), >2.5 (+2 charge) and >3.5 (+3 charge), deltaCN >0.1, a minimum of 2 peptides and a probability score lower than e^{-003}.

Ingenuity Pathway Analysis (IPA). Differentially expressed proteins were analyzed using Ingenuity Pathway Knowledge Base (Ingenuity System, Mountain View, CA) to determine their most relevant interaction networks and biological functions. The IPA algorithm proceeds by selecting the most connected protein and adding other interconnected proteins to the network. Datasets containing protein accession numbers, fold change and p-values were uploaded into the program application for the analysis. The program generates networks of these proteins using the right-tailed fisher's Exact Test, by comparing the number of proteins that participate in a given function, relative to the total number of occurrences of those

proteins in all functional annotations stored in the Ingenuity Pathways Knowledge Base, and are then ranked by score, i.e. score of 2 or higher have a 99.9% confidence level of not being randomly assembled into a network. This score was used as the cut-off for identifying protein networks or pathways.

Immunoblotting. Western blotting was performed as described previously [3, 4]. The following antibodies were used: anti-VDAC (Ab5, PC548, Calbiochem), anti-mitofilin (10179-1-AP, Proteintech) and anti-Prx-SO3 antibodies (LF-PA0005, Lab Frontier). Anti-NuMA was purchased from Pharmingen (San Diego, CA). Anti-Na+/K+ ATPase, was purchased from Upstate Biotechnology (Lake Placid, NY), anti-prohibitin-1 antibody from Research Diagnostics (Flanders, NJ). Antibodies to PKCδ (sc-937), and myoglobin (sc-8081) were obtained from Santa Cruz, phospho-PKCdelta (Thr505) antibodies were purchased from Cell Signaling Technology, Inc. (Danvers, MA, Cat# 9374).

Proton magnetic resonance spectroscopy (^{1}H-NMR). Hearts were rinsed with PBS and snap-frozen immediately in liquid nitrogen. Tissues were ground under liquid nitrogen using a mortar and pestle. Water-soluble metabolites were extracted in 6% perchloric acid (PCA) [5]. Deproteinised extracts were transferred to ice cold centrifuge tubes and centrifuged at 3000 rpm for 10 minutes at 4°C. The supernatant was transferred to fresh cold centrifuge tubes and neutralised to pH 7 with 10M KOH. After neutralization, extracts were centrifuged, the supernatant was collected, freeze-dried and reconstituted in deuterium oxide (D_2O). Immediately before the NMR analysis, the pH was readjusted to 7 with PCA or KOH. 0.5ml of the extracts were placed in 5mm NMR tubes. ^{1}H-NMR spectra were obtained using a Bruker 600MHz spectrometer. The water resonance was suppressed by using gated irradiation centred

on the water frequency. Sodium 3-trimethylsilyl-2,2,3,3-tetradeuteropropionate (TSP) was added to the samples for chemical shift calibration and quantification.

ONLINE REFERENCES

[1] Bradford MM. A rapid and sensitive method for the quantitation of microgram quantities of protein utilizing the principle of protein-dye binding. Anal Biochem. 1976 May 7; 72: 248-54.

[2] Yan JX, Wait R, Berkelman T, Harry RA, Westbrook JA, Wheeler CH, et al. A modified silver staining protocol for visualization of proteins compatible with matrix-assisted laser desorption/ionization and electrospray ionization-mass spectrometry. Electrophoresis. 2000 Nov; 21(17): 3666-72.

[3] Li C, Hu Y, Mayr M, Xu Q. Cyclic strain stress-induced mitogen-activated protein kinase (MAPK) phosphatase 1 expression in vascular smooth muscle cells is regulated by Ras/Rac-MAPK pathways. J Biol Chem. 1999; 274(36): 25273-80.

[4] Li C, Hu Y, Sturm G, Wick G, Xu Q. Ras/Rac-Dependent activation of p38 mitogen-activated protein kinases in smooth muscle cells stimulated by cyclic strain stress. Arterioscler Thromb Vasc Biol. 2000; 20(3): E1-9.

[5] Bergmeyer H. Methods of enzymatic analysis. Weinheim, Germany: Verlag Chemie; 1974.

ONLINE FIGURE LEGENDS

Online Figure 1. Changes in the proteome of PKC transgenic hearts. The user interface of the Decyder 2D software (version 6.5, GE healthcare) displays the image view (top left), the experimental design view (top right), the 3D view (bottom left) and the table view (bottom right) for "mitofilin" (A, spot no 1, online table I) and "cytoplasmic malate dehydrogenase" (B, spot no 25, online table III). Note the differential expression in constitutively active (AE) PKCε hearts (arrows), while expression levels in control and dominant negative (DN) PKCε hearts were identical. Both spots marked with arrows were identified as mitofilin on 2-DE gels, indicating a post-translational modification.

Online Figure 2. Immunoblotting. Mitochondrial extracts of controls (ctrl) and transgenic hearts with constitutive active (AE) and dominant negative (DN) PKCε were analyzed by Western blotting and probed with antibodies to manganese superoxide dismutase (MnSOD, SOD2), oxidized peroxiredoxins (Prx-SO3) and mitofilin. A moderate reduction of MnSOD expression was confirmed in AE PKCε transgenic hearts by densitometry (B). The oxidation state of mitochondrial peroxiredoxins, which contain a redox-active cystein, was not affected. No change in net expression was found for mitofilin, which is consistent with the observed acidic shift on the 2-DE gel (Online Figure 1A).

Online Figure 3. Pathway analysis for PKCε transgenic hearts. The dominant networks in AE (A) and DN PKCε hearts (B). Red and green colors indicate up- and

downregulation of protein isoforms, respectively (Supplemental Tables I-III). Note that glucose metabolism constituted a core of these protein association networks.

Online Figure 4. Principal Component Analysis. Metabolite extracts of controls (triangles) and AE PKCε transgenic hearts (circles) were analyzed by ^{1}H-NMR spectroscopy. Principal Component Analysis (PCA) was applied to investigate the variation of the samples in the metabolite space before (A) and after ischemia/reperfusion (B).

Supplemental Figure 1 Mayr et al

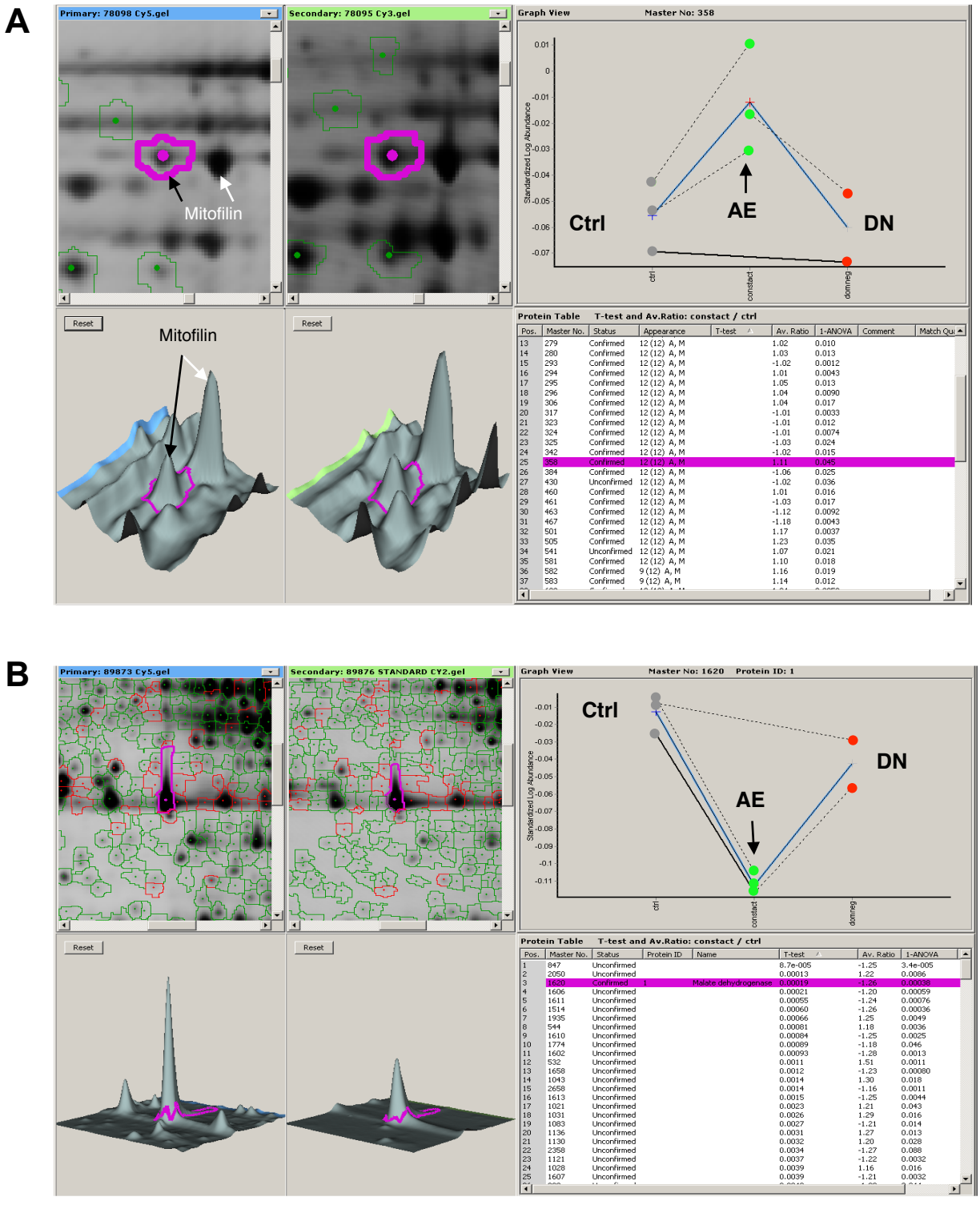

A

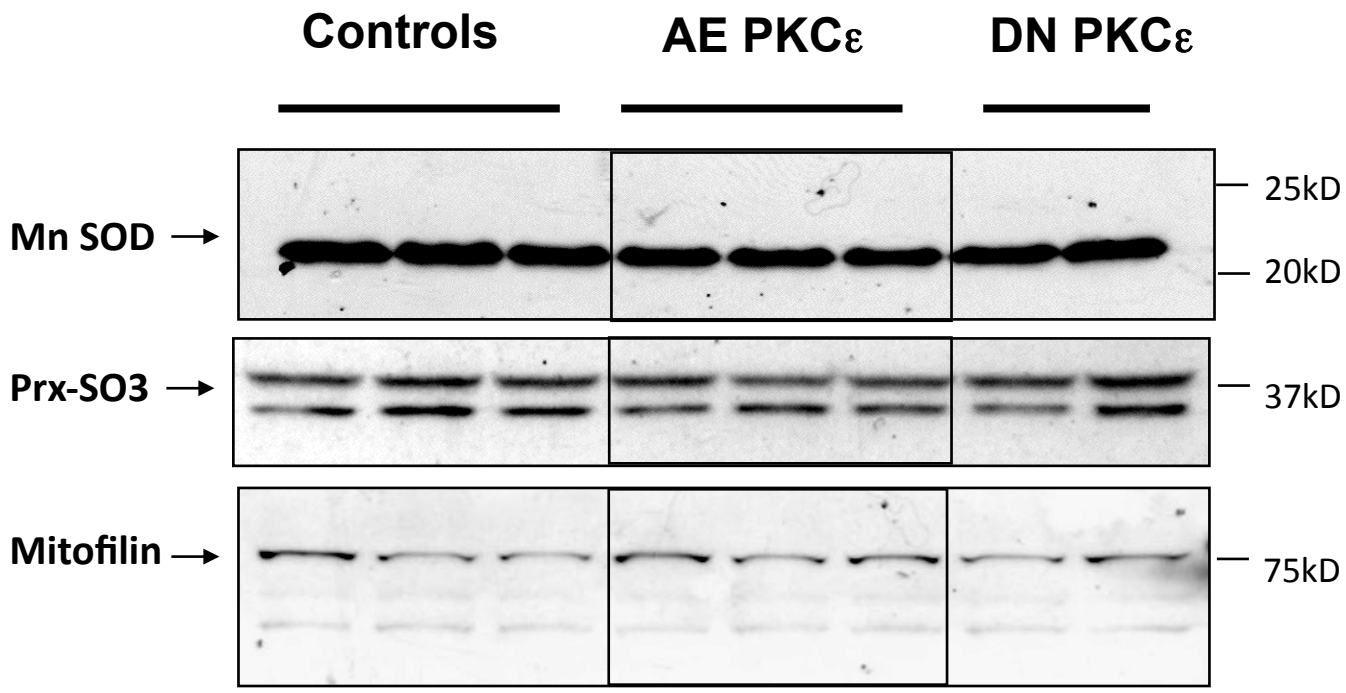
Controls
AE PKCε
DN PKCε
Mn SOD
Prx-SO3
Mitofilin
25kD
20kD
37kD
75kD

B

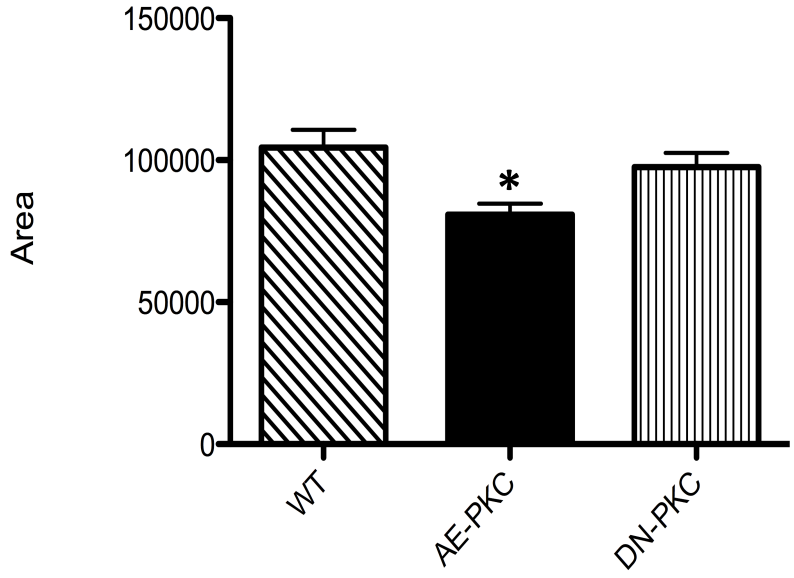
150000
100000
50000
0
Area
*
WT
AE-PKC
DN-PKC

Supplemental Figure 3

Mayr et al

A

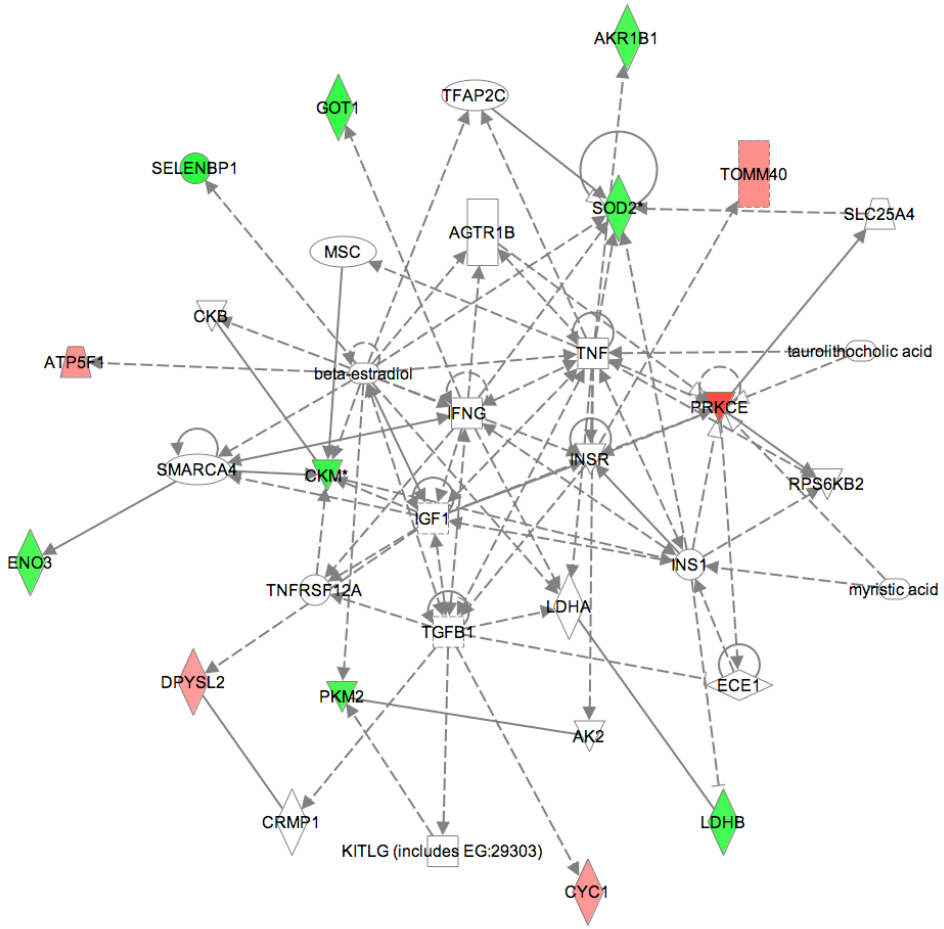

B

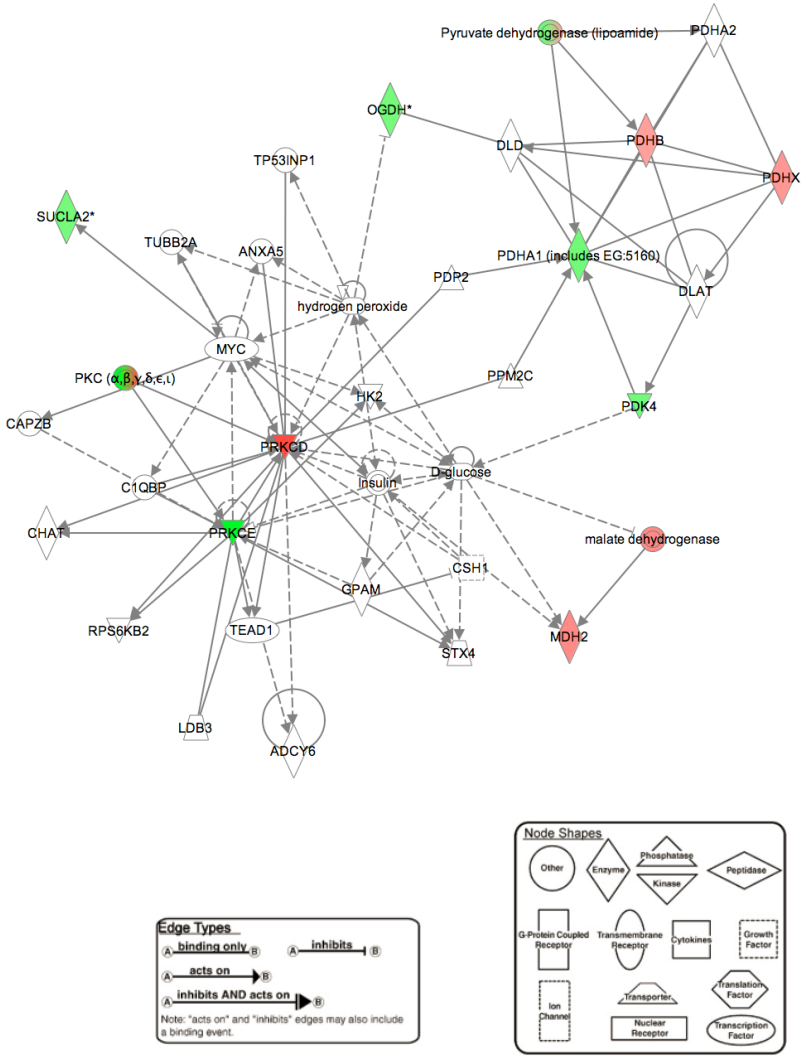

A

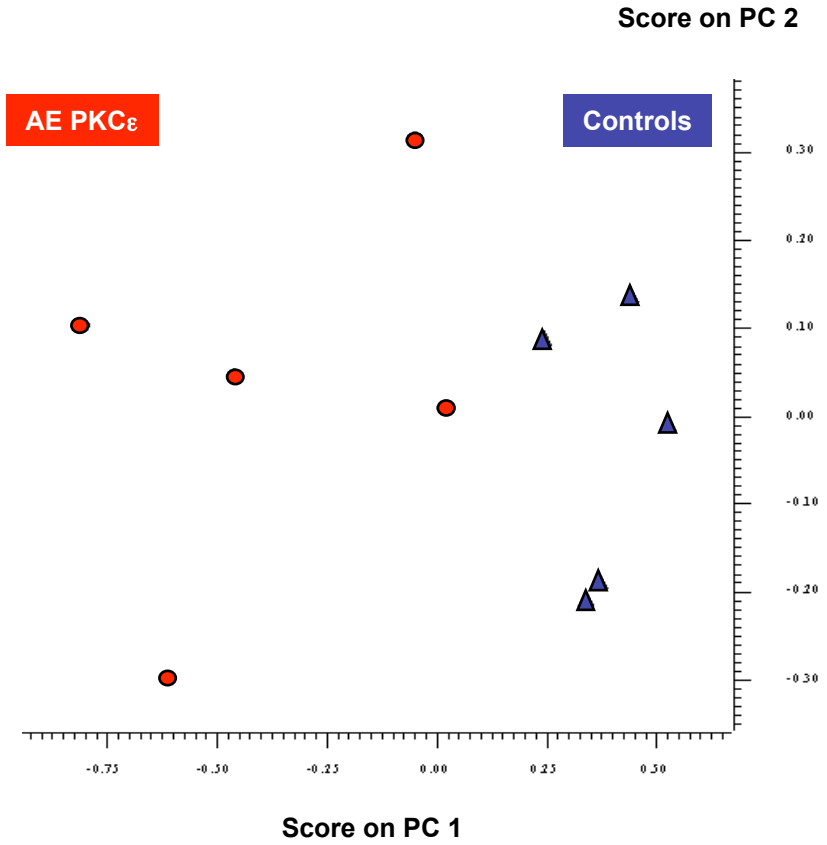
Score on PC 2
AE PKCε
Controls
0.30
0.20
0.10
0.00
-0.10
-0.20
-0.30
-0.75
-0.50
-0.25
0.00
0.25
0.50
Score on PC 1

B

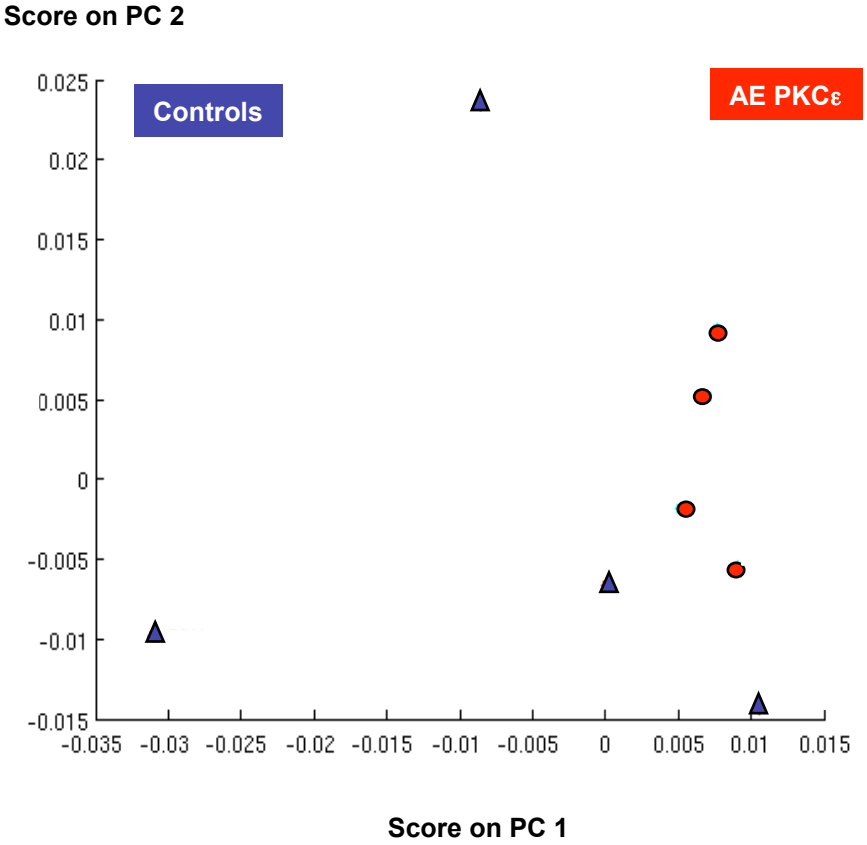
Score on PC 2
Controls
AE PKCε
0.025
0.02
0.015
0.01
0.005
0
-0.005
-0.01
-0.015
-0.035
-0.03
-0.025
-0.02
-0.015
-0.01
-0.005
0
0.005
0.01
0.015
Score on PC 1

Supplemental Table I. Differentially expressed mitochondrial proteins in transgenic hearts with constitutively active PKCepsilon (AE)

N	Protein identity	IPI Number	Theoretical pI / MW (Da x 10^3)	Coverage (% AA)	XC Score	AE *vs* Ctrl & DN	P T-test	P ANOVA
	Inner mitochondrial membrane							
1	Mitofilin	00228150	6.0 / 83.8	42.1	330.3	+1.11	0.019	0.081
	Outer mitochondrial membrane							
2	Tom 40 homolog	00135946	8.3 / 37.9	15.0	30.4	+ 1.24	0.038	0.019
	Antioxidants							
3	Manganese superoxide dismutase	00109109	8.3 / 24.6	24.8	30.3	-1.27	0.0051	0.0076
4	Manganese superoxide dismutase	00109109	8.3 / 24.6	47.3	70.3	-1.17	0.036	0.10
5	Manganese superoxide dismutase	00109109	8.3 / 24.6	42.3	65.3	-1.18	0.030	0.11
	TCA cycle							
6	Isocitrate dehydrogenase, alpha	00459725	6.0 / 39.6	9.5	20.2	-1.47	0.0015	0.011
7	Isocitrate dehydrogenase, alpha	00459725	6.0 / 39.6	20.2	80.2	-1.14	0.014	0.049
	Others							
8	Dihydropyrimidinase-like 2	00420349	6.0 / 62.2	28.3	88.3	+1.19	0.011	0.0033

Values are average ratios, XC denotes X-correlation score as calculated by the Sequest algorithm, Ctrl denotes controls, AE constitutively active, DN dominant negative PKCε transgenic hearts. Subcellular extracts were prepared from 16 murine hearts (n=6 for control and AE mice, n=4 for DN mice) with two samples being combined to obtain sufficient material for a 2-DE gel. p-values are derived from ANOVA or unpaired Student's t-test comparing AE transgenic *vs* control and DN hearts.

Supplemental Table II. Differentially expressed mitochondrial proteins in transgenic hearts with dominant negative PKCepsilon (DN)

N	Protein identity	IPI Number	Theoretical pI / MW (Da x 10^3)	Coverage (% AA)	XC Score	DN *vs* Ctrl & AE	P T-test	P ANOVA
	Glucose metabolism							
9	Mixture:							
	Pyruvate dehydrogenase, E1 alpha	00337893	8.1 / 43.2	30.5	173.5	-1.44	0.0002	0.00029
	Pyruvate dehydrogenase kinase 4	00119431	6.7 / 46.6	25.7	110.2	-1.44	0.0002	0.00029
10	Pyruvate dehydrogenase, E1 beta	00132042	6.0 / 38.9	73.3	508.3	+1.13	0.0027	0.0073
11	Pyruvate dehydrogenase, X	00222767	7.7 / 53.9	26.2	180.3	+1.19	0.025	0.093
	Lipid metabolism							
12	Hydroxysteroid dehydrogenase-like 2	00117214	6.0 / 55.6	30.1	230.3	-1.36	0.0041	0.022
13	Hydroxysteroid dehydrogenase-like 2	00117214	6.0 / 55.6	49.4	368.3	-1.39	0.0066	0.015
14	Hydroxysteroid dehydrogenase-like 2	00117214	6.0 / 55.6	46.6	218.3	-1.43	0.043	0.0077
	TCA cycle							
15	Oxoglutarate dehydrogenase, E1	00128281	6.0 / 117.7	9.9	50.3	-1.37	0.0098	0.041
16	Oxoglutarate dehydrogenase, E1	00128281	6.0 / 117.7	38.5	430.4	-1.32	0.0035	0.018
17	Succinate CoA ligase, beta subunit	00459487	6.0 / 46.8	17.1	60.2	-1.26	0.049	0.084
18	Succinate CoA ligase, beta subunit	00459487	6.0 / 46.8	17.1	60.2	-1.23	0.0081	0.033
19	Malate dehydrogenase, NAD	00331590	8.3 / 35.6	33.4	108.2	+1.22	0.093	0.030
	Others							
20	Ubiquinone methyltransferase COQ5	00379695	7.2 / 37.4	42.8	225.4	-1.21	0.0026	0.0067

For abbreviations see Supplemental Table I footnote, p-values are derived from ANOVA or unpaired Student's t-test comparing DN transgenic *vs* control and AE hearts.

Supplemental Table III. Differentially expressed cytosolic proteins in transgenic hearts with constitutively active PKCepsilon (AE)

N	Protein identity	IPI Number	Theoretical pI / MW (Da x 10^3)	Coverage (% AA)	XC Score	AE *vs* Ctrl & DN	P T-test	P ANOVA
	Glucose metabolism							
21	L-lactate dehydrogenase B chain	00229510	5.6 / 36.4	34.8	152.3	-1.18	0.022	0.019
22	Pyruvate kinase, muscle isozyme	00469199	7.2 / 57.8	34.7	238.3	-1.17	0.039	0.00046
23	Beta-Enolase	00228548	6.8 / 46.7	25.6	198.3	-1.17	0.0040	0.014
24	Aldose reductase	00223757	6.8 / 35.7	16.8	40.3	-1.16	0.025	0.060
	Malate-Asparate shuttle							
25	Malate dehydrogenase, cytoplasmic	00336324	6.2 / 36.3	42.0	130.3	-1.22	0.00051	0.0013
26	Malate dehydrogenase, cytoplasmic	00336324	6.2 / 36.3	41.4	110.3	-1.21	0.0054	0.0020
27	Aspartate aminotransferase, cytoplasmic	00230204	6.7 / 46.2	35.1	200.3	-1.23	0.022	0.023
	Energy metabolism							
28	Creatine kinase, M-type	00120076	8.4 / 47.5	43.5	298.4	-1.25	0.011	0.033
29	Creatine kinase, M-type	00120076	8.4 / 47.5	40.8	240.3	-1.18	0.044	0.029
	Mitochondrial proteins							
30	Ubiquinol Cytochrome C reductase, complex core protein 1	00111885	5.7 / 52.7	33.5	140.3	+1.15	0.049	0.032
31	ATP synthase beta chain	00468481	5.1 / 56.3	69.4	290.3	+1.16	0.031	0.012
	Antioxidant							
32	Selenium binding protein 1	00314298	5.8 / 52.7	42.6	150.3	-1.33	0.0027	0.017

For abbreviations see Supplemental Table I footnote, p-values are derived from ANOVA or unpaired Student's t-test comparing AE transgenic *vs* control and DN hearts.

Supplemental Table IV.
Metabolic effects of transgenic PKCε activation in normoxic hearts.

	Ctrl (n=5)	AE (n=5)	P (t-test)
Leucine	0.149 (±0.018)	0.098 (±0.003)	0.045
Isoleucine	0.069 (±0.018)	0.033 (±0.002)	0.109
Valine	0.203 (±0.032)	0.127 (±0.006)	0.078
Beta-hydroxybutyrate	0.207 (±0.063)	0.070 (±0.010)	0.094
Lactate	16.658 (±0.724)	11.357 (±0.624)	< 0.001
Alanine	1.776 (±0.148)	1.599 (±0.129)	0.394
Acetate	0.144 (±0.020)	0.230 (±0.095)	0.425
Glutamate	2.639 (±0.169)	3.443 (±0.194)	0.015
Succinate	1.773 (±0.437)	1.837 (±0.386)	0.916
Glutamine	6.965 (±0.562)	4.265 (±0.429)	0.006
Aspartate	0.478 (±0.040)	0.665 (±0.074)	0.066
Choline	0.190 (±0.029)	0.361 (±0.018)	0.002
Phosphocholine	0.227 (±0.023)	0.178 (±0.023)	0.168
Carnitine	0.722 (±0.092)	0.618 (±0.054)	0.364
Taurine	35.052 (±0.735)	30.191(±1.729)	0.046
Glucose	0.961 (±0.198)	0.312 (±0.073)	0.027
Fumarate	0.156 (±0.032)	0.098 (±0.016)	0.155
Tyrosine	0.091 (±0.011)	0.069 (±0.006)	0.108
Total creatine	13.034 (±0.591)	10.767 (±0.762)	0.048
Phenylalanine	0.092 (±0.007)	0.074 (±0.005)	0.080
Adenosine nucleotides	2.848 (±0.201)	4.307 (±0.432)	0.024
Glycolic acid	0.696 (±0.171)	0.647 (±0.036)	0.795
Glycine	0.833 (±0.045)	0.779 (±0.091)	0.611
NAD+NADH	0.077 (±0.011)	0.320 (±0.112)	0.096
Formate	0.124 (±0.046)	0.163 (±0.041)	0.549

Data presented are given in μmol/g wet weight (mean±SE), P-values were derived from unpaired Student's t-test

Supplemental Table V.
Metabolic effects of transgenic PKCε activation in ischemic hearts.

	Ctrl (n=4)	AE (n=3)	P (t-test)
Leucine	0.183 (±0.043)	0.146 (±0.018)	0.46
Isoleucine	0.253 (±0.009)	0.264 (±0.044)	0.83
Valine	0.177 (±0.032)	0.224 (±0.059)	0.53
Beta-hydroxybutyrate	0.058 (±0.013)	0.079 (±0.029)	0.55
Lactate	4.084 (±0.798)	4.768 (±2.946)	0.84
Alanine	1.511 (±0.114)	1.762 (±0.214)	0.37
Acetate	0.427 (±0.155)	0.618 (±0.186)	0.47
Glutamate	1.917 (±0.147)	1.610 (±0.156)	0.21
Succinate	1.027 (±0.068)	1.026 (±0.363)	1.00
Glutamine	3.763 (±0.425)	3.623 (±0.245)	0.79
Aspartate	0.433 (±0.047)	0.400 (±0.073)	0.73
Choline	0.200 (±0.052)	0.147 (±0.028)	0.41
Phosphocholine	0.144 (±0.031)	0.137 (±0.007)	0.83
Carnitine	0.560 (±0.148)	0.760 (±0.132)	0.36
Taurine	22.966 (±2.717)	24.044 (±1.611)	0.75
Glucose	0.487 (±0.109)	0.599 (±0.168)	0.61
Fumarate	0.021 (±0.005)	0.041 (±0.026)	0.52
Tyrosine	0.049 (±0.013)	0.031 (±0.009)	0.31
Total creatine	9.630 (±0.994)	8.281 (±1.242)	0.44
Phenylalanine	0.065 (±0.010)	0.052 (±0.008)	0.34
Adenosine nucleotides	3.625 (±0.396)	3.801 (±0.221)	0.72
Glycolic acid	0.594 (±0.047)	0.658 (±0.063)	0.46
Glycine	0.633 (±0.048)	0.601 (±0.010)	0.56
NAD+NADH	0.498 (±0.081)	0.330 (±0.137)	0.36
Formate	0.349 (±0.130)	0.382 (±0.141)	0.87

See legend to Supplemental Table IV

Supplemental Table VI.
Metabolic effects of transgenic PKCε in reperfused hearts.

	Ctrl (n=4)	AE (n=4)	DN (n=4)	P (Anova)
Leucine	0.150 (±0.003)	0.155 (±0.009)	0.163 (±0.010)	0.509
Isoleucine	0.221 (±0.029)	0.315 (±0.028)*	0.109 (±0.026)	0.002
Valine	0.150 (±0.004)	0.175 (±0.014)	0.113 (±0.041)	0.271
Beta-hydroxybutyrate	0.036 (±0.007)	0.092 (±0.044)	0.043 (±0.005)	0.303
Lactate	1.688 (±0.402)	2.836 (±0.497)*	0.885 (±0.240)	0.020
Alanine	1.288 (±0.169)	2.443 (±0.306)**	0.883 (±0.077)	0.001
Acetate	0.430 (±0.173)	0.262 (±0.106)	0.182 (±0.059)	0.381
Glutamate	1.188 (±0.181)	1.729 (±0.131)	1.176 (±0.161)	0.059
Succinate	0.744 (±0.053)	1.053 (±0.159)	0.635 (±0197)	0.176
Glutamine	2.913 (±0.300)	4.172 (±0.210)*	2.505 (±0.445)	0.016
Aspartate	0.299 (±0.061)	0.581 (±0.052)**	0.292 (±0.050)	0.007
Choline	0.162 (±0.007)	0.180 (±0.006)	0.294 (±0.143)	0.500
Phosphocholine	0.107 (±0.030)	0.153 (±0.017)	0.826 (±0.315)	0.038
Carnitine	0.586 (±0.067)	0.792 (±0.046)	0.639 (±0.280)	0.677
Taurine	18.449(±2.145)	25.847 (±1.436)**	17.06 (±1.159)	0.009
Glucose	0.650 (±0.223)	0.972 (±0.171) *	0.195 (±0.062)	0.027
Fumarate	0.021 (±0.007)	0.029 (±0.007)	0.014 (±0.005)	0.357
Tyrosine	0.043 (±0.007)	0.046 (±0.007)	0.026 (±0.005)	0.111
Total creatine	6.707 (±1.073)	8.402 (±0.223)	6.659 (±0.407)	0.171
Phenylalanine	0.062 (±0.006)	0.060 (±0.004)	0.061 (±0.014)	0.993
Adenosine nucleotides	2.764 (±0.285)	3.843 (±0.282)**	2.473 (±0.164)	0.009
Glycolic acid	0.602 (±0.056)	0.626 (±0.053)	0.535 (±0.139)	0.776
Glycine	0.547 (±0.031)	0.731 (±0.090)*	0.367 (±0.095)	0.028
NAD+NADH	0.428 (±0.040)	0.585 (±0.018)**	0.328 (±0.024)	0.001
Formate	0.343 (±0.136)	0.230 (±0.086)	0.115 (±0.007)	0.273

Data presented are given in μmol/g wet weight (mean±SE), differences from all groups were derived from ANOVA tables, * statistically significant difference from DN hearts, ** statistically significant difference from control as well as DN hearts